ANALYSIS OF HIGH EFFICIENCY IN TERAHERTZ QUANTUM CASCADE LASER

R.NIRANJANA R.A.ROSHINI P.ASHOK

Student, ECE, Prince Shri Venkateshwara Padmavathy Engineering College, Tamilnadu, India
Student, ECE, Prince Shri Venkateshwara Padmavathy Engineering College, Tamilnadu, India
Assistant professor, ECE, Prince Shri Venkateshwara Padmavathy Engineering College, Tamilnadu, India

ABSTRACT

Terahertz quantum cascade laser is used for wide range of new applications.A device-specific model was developed in order to predict the optical output power under changing temperature.Model parameters are deduced from the rate equation, obtained from Schrodinger-Poisson scattering calculations.The model is being condensed by fitting the polynomials to data arrays and represents the rate equation parameters.By condensing the model, memory usage and computational efficiency is been increased.

Keyword: *Quantum cascade laser, thermal roll over, dynamic characteristics, reduced rate equation.*

1. INTRODUCTION

Terahertz quantum cascade laser are powerful radiation sources for high resolution and high sensitivity spectroscopy with a discrete spectrum between 2 and 5 THz as well as a continuous coverage of several GHz.It is a radiation source with a continuous coverage of substantially larger frequency range.Multi mode THz QCL was operated with a fast ramped injection current.The exact range of temperature and the voltage at which the maximum power can be obtained is not known.The dynamic behavior that is both temperature and time dependent and the maximum efficiency values are determined.

2. REDUCED RATE EQUATIONS

$$\frac{dS(t)}{dt} = -\frac{1}{\tau p}S(t) + \frac{\beta sp}{\tau sp(T,V)}N3(t) + MG(T,V)\frac{(N3(t)-N2(t))}{1+\varepsilon S(t)}S(t) \quad (1)$$

$$\frac{dN3(t)}{dt} = -G(T,V)\frac{(N3(t)-N2(t))}{1+\varepsilon S(t)}S(t)\ N3(t) - \frac{1}{\tau 3(T,V)}N3(t) + \frac{\eta 3(T,V)}{q}I(t) \quad (2)$$

$$\frac{dN2(t)}{dt} = +G(T,V)\frac{((N3(t)-N2(t))}{1+\varepsilon S(t)}S(t) + \frac{1}{\tau 32(T,V)}N3(t) + \frac{\eta 2(T,V)}{q}I(t) - \frac{1}{\tau 21(T,V)}N2(t) \quad (3)$$

$$\frac{dT(t)}{dt} = \frac{1}{mcp}(I(t)V(T(t),I(t)) - \frac{(T(t)-T0)}{Rth}) \quad (4)$$

The symbol S(t) represents photon population, τp the photon lifetime in the cavity, $N_3(t)$ the ULL carrier number, $N_2(t)$the LLL carrier number, I(t) the current forcing function, q the electronic charge, $\beta_{sp}$the spontaneous emission factor, $\tau_{sp}$the spontaneous emission lifetime (or radiative spontaneous relaxation time), and M is the number of periods in the structure, 90 in the case of our exemplar QCL. The η_3 term in Eq. (1.2) models carrier injection efficiency into the ULL and the η_2 term in Eq. (1.3) models carrier injection efficiency directly into the LLL. The carrier lifetime for non-radioactive transitions from the ULL to LLL is τ_{32}, the total lifetime due to non-radiative transitions for the ULL carrier population is τ_3, and the lifetime for transitions from the LLL to the continuum is τ_{21}. The gain factor is represented by G, voltage V and temperature T are themselves time-dependent, but for the sake of readability are not written explicitly as functions of time.

$$P(t)=\eta 0\hbar\omega S(t)/\tau_p$$

where η0 is the power output coupling efficiency, $\hbar$ is the reduced Planck constant, and ω is the laser's angular emission frequency.

The general third order polynomial equation is

$$Z(T,V)=a00+a10T+a01V+a11TV+a20T2+a02V2+a21T2V+a12TV2+a30T3+a03V3$$

Terminal voltage V(t) was modeled by fitting a third order polynomial of the following form to measured temperature-dependent current–voltage data

$$V(I,T)=a00+a10I+a01T+a11IT+a20I2+a02T2+a21I2T+a12IT2+a30I3+a03T3$$

.

2.1 IV CHARACTERISTICS

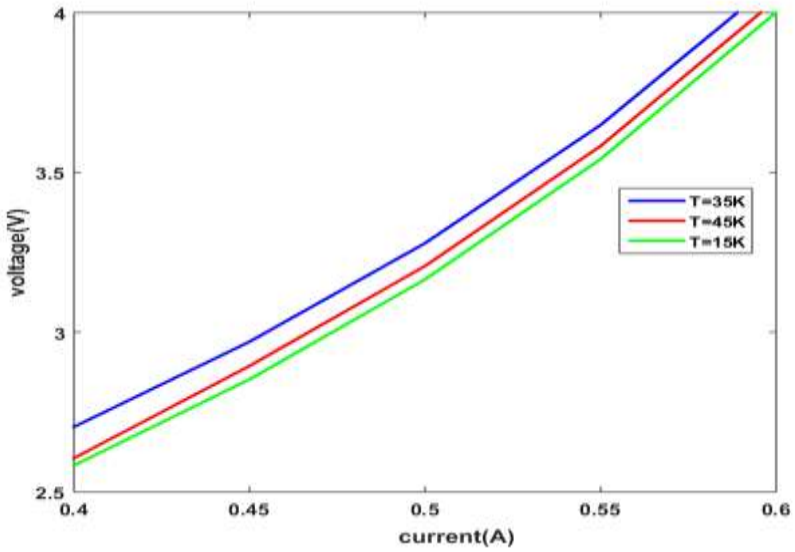

Fig 1 IV Characteristics

Fig 1 indicates the current ranges over which the QCL does not lase. Although the RREs are expressed in terms of a current forcing function I(t), terminal voltage V(t)is also required by the equations for two reasons:

(i) calculation of self heating within the AR

(ii) calculation of each of the ever-changing voltage-dependent RRE parameters. With I(t) as the independent variable, V(t) may be calculated from the temperature-dependent current–voltage (IV) characteristics of the QCL, shown in Fig. 2. This can be done via a behavioral model of V(t) expressed in terms of I(t) and T(t) . QCLs have IV characteristics somewhat different to, and more difficult to model theoretically, than those of diode lasers. For maximum accuracy we opted for a behavioral model based on measured temperature-dependent IV data, rather than use theoretically predicted IV characteristics.

2.2 THERMAL ROLLER

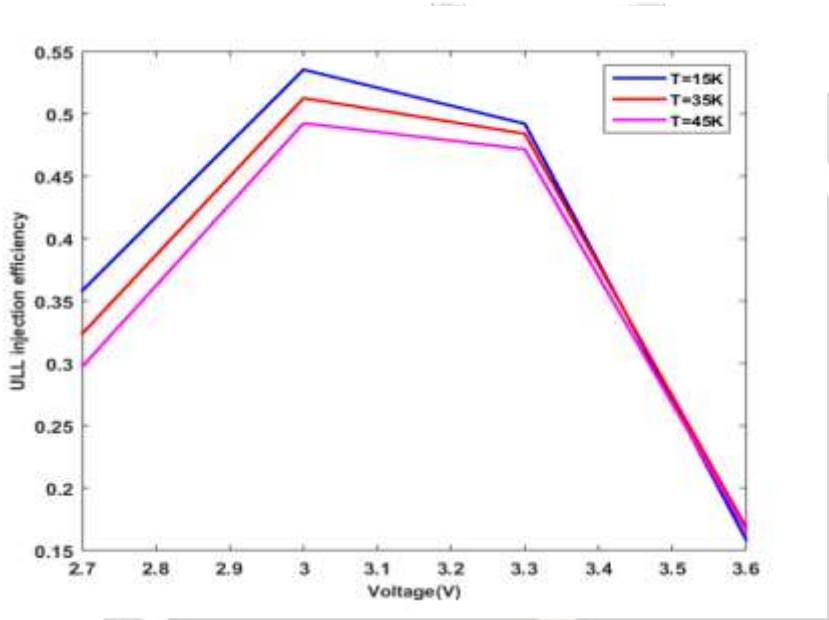

Fig -2 Thermal Roller

Figure 2 represents η_3 as a surface, showing temperature and voltage dependence. Fall off in η_3 with increasing drive current occurs much more rapidly with voltage than temperature making it the primary cause of roll-over in this QCL. It shows the polynomial coefficients can be viewed as a compressed form of the full RRE data, and polynomials present the additional benefit of de-noising and smoothing the bulk data an important consideration in solving a set of stiff differential equations.

3. EFFECT OF RRE PARAMETERS

The model predicts the exemplar QCL's LI characteristics by excitation with a slow current ramp I(t) from 300 to 600 mA. The timescale of the ramp 1s was far beyond that of the laser's electro-optic and thermal dynamics, giving a result that well represents the static response. The simulation was repeated for three cold finger temperatures, T_0 = 15 K, 35 K, and 45 K, producing the results.

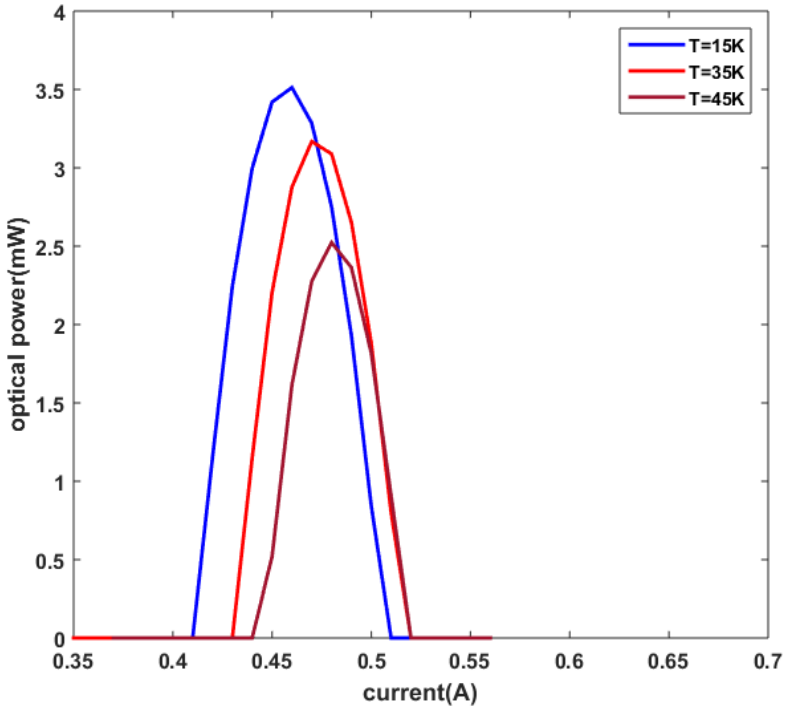

Fig -3 Steady State characteristics independent of Voltage

The Figure 3 represents the effect of RRE parameter voltage-dependence on L-I characteristics. L-I simulations with voltage dependent RRE parameters at T_0=15 K, 35 K and 45 K. are measured. Characteristics of the QCL at some of the same temperatures, vertically scaled by a factor of approximately four to compensate for the poor efficiency of the collection equipment.

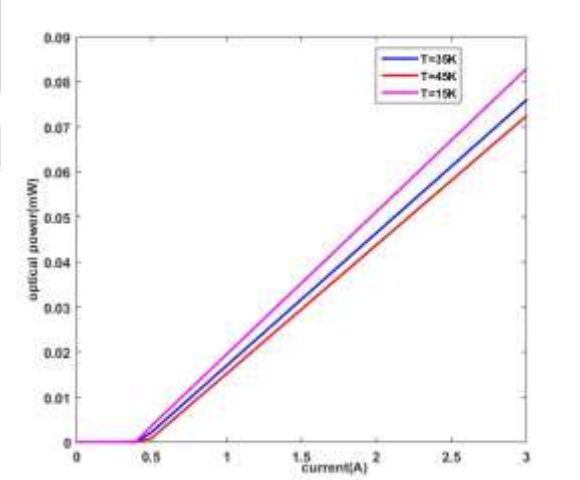

Fig -4 . Steady State characteristics dependent of voltage

The figure 4 represents the Effect of cold finger temperature on step response. Response of the QCL to a current step of 0.470 A for six cold finger temperatures with both temperature- voltage-dependence of RRE parameters invoked. Both turn-on delay and pulse rise times increase with increasing cold finger temperature.

4. STATIC BEHAVIOUR

The physical cause of voltage-related roll-over is a misalignment between the injector and ULL at higher voltages that manifests as a rapid drop in injection efficiency η_3. The figure clearly shows that near roll-over η_3 drops far more rapidly due to voltage change.

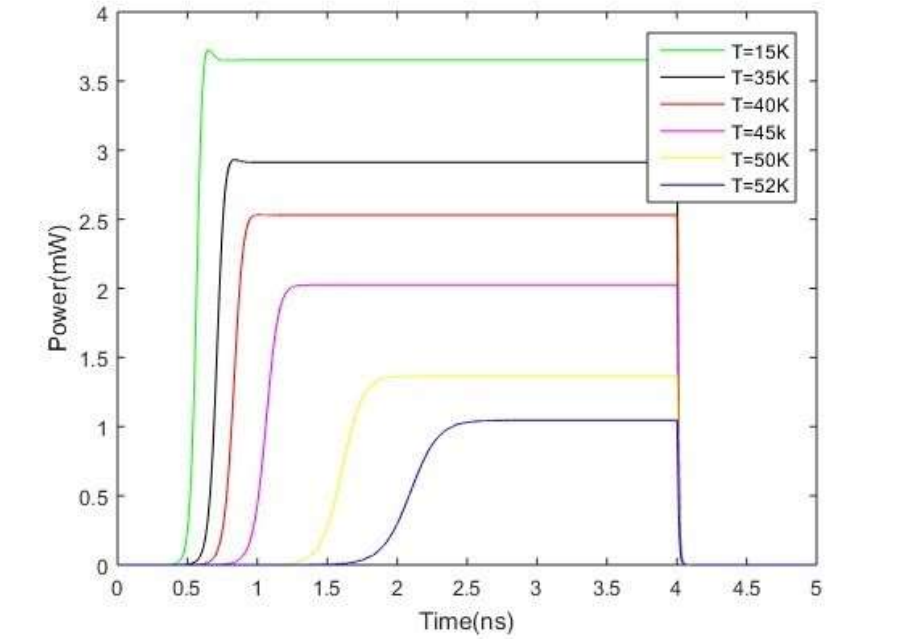

Fig-5 Turn on Delay and Pulse Rise Time with Increase in Temperature

The Figure 5 represents the effect of cold finger temperature on step response. Response of the QCL to a current step of 0.470 A for six cold finger temperatures (colour online) is shown, with both temperature- voltage-dependence of RRE parameters invoked. Both turn-on delay and pulse rise times increase with increasing cold finger temperature.

4.1. VARYING OF VALUE OF CURRENT AGAINST TEMPERATURE

Cold is the presence of low temperature A lower bound to temperature is absolute zero, defined as 0.00 K on the Kelvin scale, an absolute thermodynamic temperature scale. Cold fingers can be cooled to a lower temperature of −78 °C .The lower temperature achieved reduces the quantity of volatile material exhausted into the air.

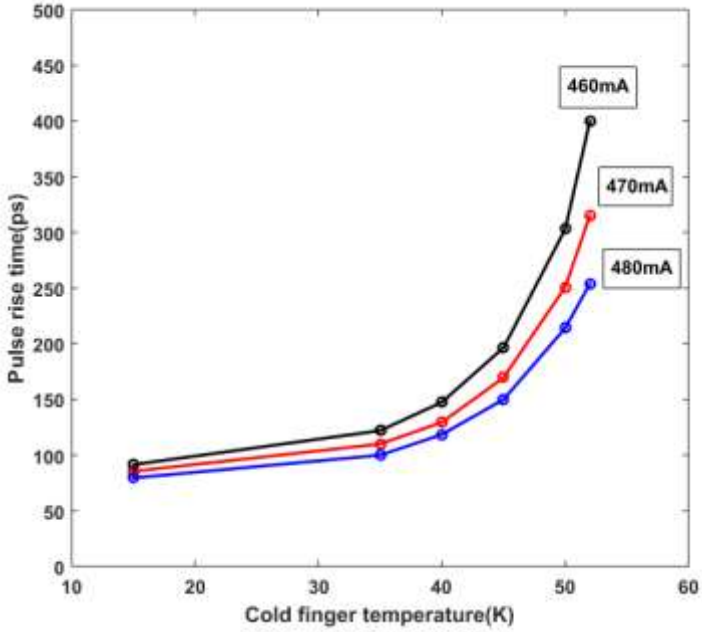

Fig -6 Pulse Rise Time Vs Temperature

The trend of rise time with temperature for 470 mA rectangular current pulses is shown in Figure 6. The simulation to study rise time against temperature at pulse amplitudes of 460 mA and 480 mA .Both turn-on delay and rise time are seen to increase non-linearly with increasing temperature, while the steady-state optical output power decreases and ceases altogether at ~53 K.

4.2. VARYING VALUE OF CURRENT AGAINST RISE TIME

The turn-on delay was derived as the time difference between the rise-up of the pump current pulse measured at the laser diode and that of the signal from the photo detector.

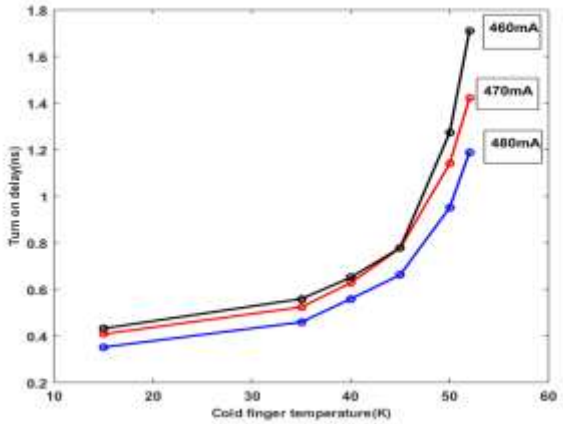

Fig -7 Turn on Delay Vs Temperature

Turn-on delay was calculated for all simulations and is seen to correlate with rise time, as shown in Figure 7 The sharp increase in both rise time (describing the speed of the system approaching saturation) and delay time (required for spontaneous emission to build up to a noticeable comes from the fast decrease of small-signal gain as the temperature increases. The results demonstrate a significant difference when voltage is not taken into account, and agree only near the temperature at which the terminal voltage is actually 3.00 V.

4.3. DYNAMIC BEHAVIOR

The effects of temperature and voltage dependence on device behaviour and demonstrate the importance of modelling voltage-dependent device behaviour. The basic dynamic behaviours that would be of interest in high speed applications, namely turn-on delay, rise time and overshoot in response to current-step excitation.

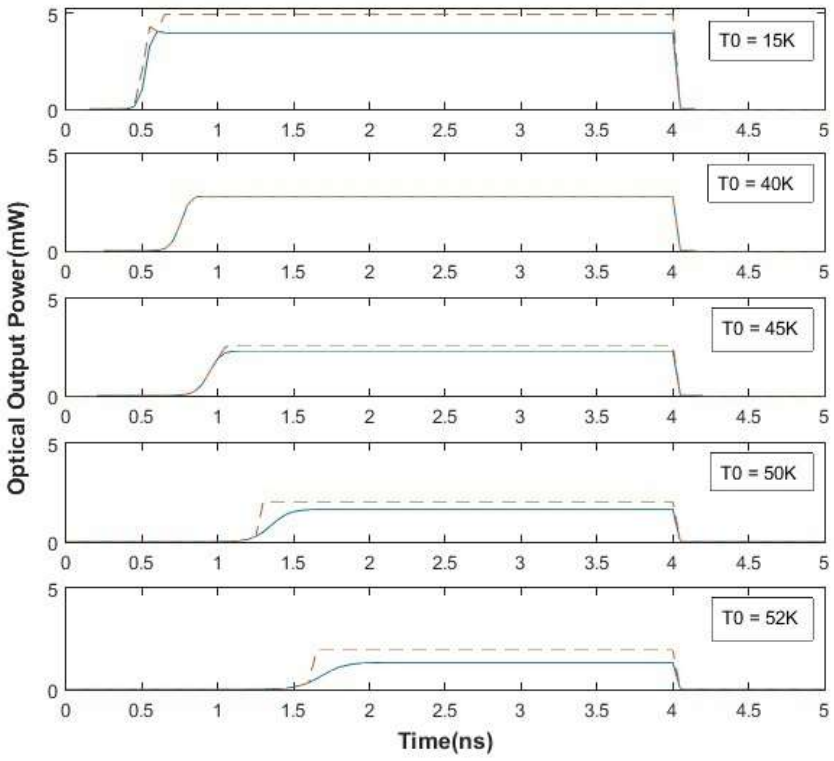

Fig -8 Effect of Cold Finger Temperature

The Figure 8 explains the effect of cold finger temperature on 0.47 A step current response when voltage-dependence of RRE parameters is suppressed (values fixed for V = 3.00 V) shown as dashed lines. For reference, solid lines (identical to those of Fig. 5) are responses with voltage-dependence invoked. Temperature and voltage-dependence of RRE parameters is thus seen to have a significant effect on both turn-on delay and pulse rise time.

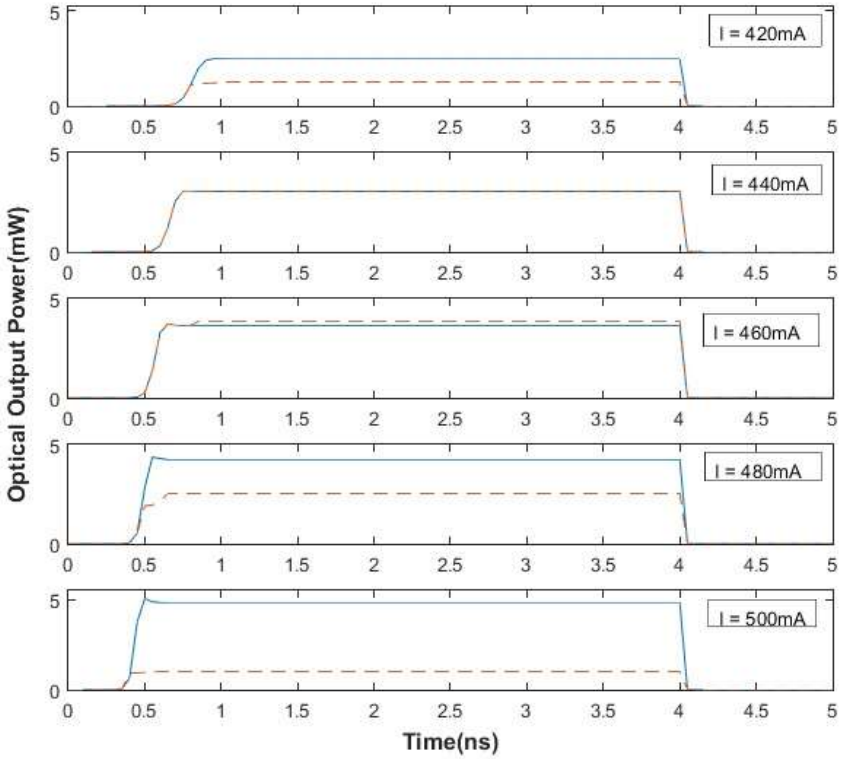

Fig -9 Effect of RRE Parameters

Figure 9 show QCL's response to five rectangular current pulses of amplitude 420, 440, 460, 480, and 500 mA. Solid lines represent the response with voltage dependence of RRE parameters invoked and broken lines the response for voltage-dependence suppressed (for constant V = 3.00 V). The peak optical power shown by the solid curves is seen to first rise and then fall, in accordance with the roll-over mechanism

5. CONCLUSION

The paper represents dynamic model of aTeraHertz QCL that behaves over a wide range of voltages and temperatures . Our simulation reveals temperature and biased dependent in turn on characteristics that would be high in free space communication and pulsed application. It demonstrates the importance of voltage and temperature dependent modelling which has an impact on device behaviour on time scale from picoseconds to static. RRE parameters are used which are the functions of device voltage and lattice temperature. RRE model is obtained which is valid over broad range of device temperature and voltages derived from the full set of RE equations. The generic approach maybe applied to any QCL by extracting appropriate parameters from a full RE model.

6. REFERENCE

1. Capasso .F, (2002) 'Quantum cascade lasers: Ultrahigh-speed operation optical wireless communication narrow line width and far-infrared emission', IEEE J. Quantum Electron., vol. 38, no. 6, pp. 511-532.

2. Fathololoumi .A, (2012) 'Terahertz quantum cascade lasers operating up to 200 k with optimized oscillator strength and improved injection tunneling', Opt. Express, vol. 20, no. 4, pp. 3866-3876.

3. Hamadou .A, Thobel .J .L, and Lamari .S, (2008) 'Modelling of temperature effects on the characteristics of mid-infrared quantum cascade lasers', Opt. Commun., vol. 281, no. 21, pp. 5385–5388.

4. Martini .R, (2002) 'Free-space optical transmission of multimedia satellite data streams using mid-infrared quantum cascade lasers', Electron. Lett., vol. 38, no. 4, pp. 181-183.

5. Petitjean .Y, Destic .F, Mollier .J .C, and Sirtori .C, (2011) 'Dynamic modeling of terahertz quantum cascade lasers', IEEE J. Sel. Topics Quantum Electron., vol. 17, no. 1, pp. 22–29.

6. Rakic .A .D, (2013) 'Swept-frequency feedback interferometry using terahertz frequency QCLs: A method for imaging and materials analysis', *Opt. Express*, vol. 21, no. 19, pp. 22194-22205.

7. Tober .R .L, (2007) 'Active region temperatures of quantum cascade lasers during pulsed excitation', J. Appl. Phys., vol. 101, Art. no. 044507.

8. Vitiello .M .S, Scamarcio .G, and Spagnolo .V, (2008) 'Time-resolved measure-ment of the local lattice temperature in terahertz quantum cascade lasers', Appl. Phys. Lett., vol. 92, no. 10, Art. no. 101116.

9. Wienold .M, (2014) 'High-temperature continuous-wave operation of terahertz quantum-cascade lasers with metal-metal waveguides and third-order distributed feedback', Opt. Express, vol. 22, no. 3, pp. 3334-3348.